Energy spectra of electrons quasi-elastically backscattered from solid surfaces

2004 J. Phys. D: Appl. Phys. 37 1394

(http://iopscience.iop.org/0022-3727/37/9/014)

INSTITUTE OF PHYSICS PUBLISHING JOURNAL OF PHYSICS D: APPLIED PHYSICS
J. Phys. D: Appl. Phys. **37** (2004) 1394–1399 PII: S0022-3727(04)69097-8

Energy spectra of electrons quasi-elastically backscattered from solid surfaces

C M Kwei[1,3], Y C Li[1] and C J Tung[2]

[1] Department of Electronics Engineering, National Chiao Tung University, Hsinchu 300, Taiwan
[2] Department of Nuclear Science, National Tsing Hua Univeristy, Hsinchu 300, Taiwan

E-mail: cmkwei@mail.nctu.edu.tw

Received 18 September 2003
Published 14 April 2004
Online at stacks.iop.org/JPhysD/37/1394
DOI: 10.1088/0022-3727/37/9/014

Abstract
The energy distribution of electrons quasi-elastically backscattered from solids has been investigated. Monte Carlo (MC) simulations were performed for the study of the recoil energy shift and the broadening of this distribution for backscattered electrons from Si and Au. In these simulations, electron interaction cross sections were obtained from calculations based on the dielectric response theory for inelastic interactions, including volume and surface excitations, and elastic interactions. The depth-dependent electron inelastic mean free path for volume excitations and the probability of surface excitations were calculated using the dielectric functions derived from optical data. The relativistic partial-wave expansion method was applied to calculate the elastic scattering cross section for a potential of the atom in the solid. The Rutherford-type recoil energy was included in the MC simulations by either considering or neglecting the thermal effect of atomic vibrations. Such an effect was applied using the single scattering model. The intensity of electrons quasi-elastically backscattered from Si and Au was simulated for incident electrons of an energy distribution. The adjustment for the spectrometer energy resolution was allowed. An analytic expression for the intensity of backscattered electrons by a single scattering was derived explicitly. A comparison of simulated results with experimental data was made and discussed.

1. Introduction

It is important to analyse the elastic peaks in the spectra of electrons backscattered from solid surfaces for many applications of surface sensitive electron spectroscopies [1, 2]. Significant information can be extracted from these analyses. In the case of elastic peak electron spectroscopy (EPES), for instance, electron inelastic mean free paths in solids can be determined [3–8]. In the analyses of elastic peaks, not only the angular distribution, but also the energy distribution characterizes the features of the spectra of backscattered electrons. The energy distribution results from the Rutherford-type recoil energy losses by electrons in the elastic interactions with atomic nuclei [9]. Such losses are very small but not negligible [10], so they are referred to as quasi-elastic recoil losses. The small energy shift and the energy broadening of quasi-elastically backscattered electrons have been observed experimentally using electron spectrometers for solids especially composed of low atomic numbered elements [9–12].

The aim of this work was to study the energy distribution of electrons quasi-elastically backscattered from solid surfaces. Quantitative analyses of experimental data on the elastic peaks were made by Boersch *et al* [9] based on the single scattering model. This model considered only a single elastic interaction in the interpretation of quasi-elastic recoil losses. Therefore, the model did not produce correctly the energy broadening and the peak shape of the elastic peak

[3] Author to whom any correspondence should be addressed.

spectrum. Since quasi-elastically backscattered electrons were contributed by single and plural elastic interactions [13], Monte Carlo (MC) simulations [13–22] were applied in this work to compute the energy distribution of electrons quasi-elastically backscattered from Si and Au surfaces. In these simulations, electron interaction cross sections were obtained from calculations based on the dielectric response theory for inelastic interactions, including volume and surface excitations, and elastic interactions. The depth-dependent electron inelastic mean free path for volume excitations [16, 23] and the probability of surface excitations [24] were calculated using the dielectric functions derived from optical data [25]. The relativistic partial-wave expansion method [22] was applied to calculate the elastic scattering cross section for a potential of the atom in the solid. This method was better than the Mott formula for elastic scattering cross sections since the Mott theory was valid only for low-Z materials [26] and considered no screening effect due to atomic electrons in the solid. The Rutherford-type recoil energy [9] was included in the MC simulations by either considering or neglecting the thermal effect of atomic vibrations. The intensity of electrons quasi-elastically backscattered from Si and Au was simulated by the consideration of the spectrometer energy resolution and the energy distribution of the primary electrons [27–29]. A comparison of simulated results with experimental data was made and discussed.

2. Theory

Electrons impinging on a solid cause elastic and inelastic interactions when they travel across the surface and inside the solid. Elastic interactions lead, primarily, to angular deflections that alter the directions of electron movements. Inelastic interactions, on the other hand, are mainly responsible for the energy loss of electrons. Inelastic interactions are comprised of volume and surface excitations. Volume excitations, including volume plasmon generations and interband transitions [25], occur predominantly as electrons travel deep inside the solid. Surface excitations [24], on the contrary, are most probable as electrons move close to the surface.

2.1. Elastic and inelastic cross sections

The differential elastic cross section per atom is given by the partial-wave expansion method as

$$\frac{\mathrm{d}\sigma_\mathrm{e}}{\mathrm{d}\Omega} = \left|\frac{1}{2\mathrm{i}K}\sum_{\ell=0}^{\infty}[(\ell+1)(\mathrm{e}^{2\mathrm{i}\delta_\ell^+}-1)+\ell(\mathrm{e}^{2\mathrm{i}\delta_\ell^-}-1)P_\ell(\cos\theta)]\right|^2 + \left|\frac{1}{2\mathrm{i}K}\sum_{\ell=1}^{\infty}(\mathrm{e}^{2\mathrm{i}\delta_\ell^-}-\mathrm{e}^{2\mathrm{i}\delta_\ell^+})P_\ell^1(\cos\theta)\right|^2, \quad (1)$$

where K is the wavenumber of the electron, θ is the scattering angle, Ω is the solid angle, δ_ℓ is the phase shift, ℓ is the quantum number of the orbital angular momentum, $\delta_\ell^\pm$ are the corresponding phase shifts for spin up and spin down, and P_ℓ and P_ℓ^1 are the Legendre and the associated first-order Legendre polynomials, respectively. To determine the phase shifts, a finite difference technique may be applied to solve the Dirac equations using the Hartree–Fock–Wigner–Seitz potential for the atom in the solid. The elastic mean free path of electrons is given by

$$\lambda_\mathrm{e} = (N\sigma_\mathrm{e})^{-1}, \quad (2)$$

where N is the atomic density of the solid, σ_e is the total elastic cross section obtained from

$$\sigma_\mathrm{e} = \int \frac{\mathrm{d}\sigma_\mathrm{e}}{\mathrm{d}\Omega}\,\mathrm{d}\Omega, \quad (3)$$

and $\mathrm{d}\Omega = \sin\theta\,\mathrm{d}\theta\,\mathrm{d}\phi$ is the differential solid angle.

The inelastic inverse mean free paths of injected (from vacuum to solid) and ejected (from solid to vacuum) electrons are given by

$$[\lambda_i^{\mathrm{v}\to\mathrm{s}}(E,z)]^{-1} = \mu_i^{\mathrm{v}\to\mathrm{s}}(E,z) = \int_0^E \mu_i^{\mathrm{v}\to\mathrm{s}}(E,\omega,z)\,\mathrm{d}\omega \quad (4)$$

and

$$[\lambda_i^{\mathrm{s}\to\mathrm{v}}(E,z)]^{-1} = \mu_i^{\mathrm{s}\to\mathrm{v}}(E,z) = \int_0^E \mu_i^{\mathrm{s}\to\mathrm{v}}(E,\omega,z)\,\mathrm{d}\omega, \quad (5)$$

where E, ω, and z are, respectively, the energy, energy loss, and depth of electrons. Note that these differential and total inelastic inverse mean free paths depend on the depth of electrons in the solid. When electrons travel inside the solid but near the surface, surface excitations dominate the contribution to the inelastic inverse mean free path. On the contrary, volume excitations dominate this contribution as electrons move deep inside the solid. The sum of surface and volume inelastic inverse mean free paths is, however, roughly depth-independent at any depths [24] due to the approximate compensation of volume and surface excitations at any depths. As electrons travel outside the solid but close to the surface, the inelastic inverse mean free path is only contributed by surface excitations. To characterize the probability of surface excitations, one generally uses the surface excitation parameter defined by

$$P_\mathrm{s}^{\mathrm{v}\to\mathrm{s}}(E) = \int_{-\infty}^0 \mathrm{d}z \int_0^E \mu_i^{\mathrm{v}\to\mathrm{s}}(E,\omega,z)\,\mathrm{d}\omega \quad (6)$$

for electrons moving from vacuum to a semi-infinite solid at $z > 0$, and

$$P_\mathrm{s}^{\mathrm{s}\to\mathrm{v}}(E) = \int_{-\infty}^0 \mathrm{d}z \int_0^E \mu_i^{\mathrm{s}\to\mathrm{v}}(E,\omega,z)\,\mathrm{d}\omega, \quad (7)$$

for electrons moving from solid to vacuum.

Models for calculating the elastic cross sections, inelastic inverse mean free paths for volume excitations and inelastic surface excitation parameters have been developed previously. A detailed description of these models is given elsewhere [24]. In this work, the elastic cross sections were determined using the partial-wave expansion method with the Hartree–Fock–Wigner–Seitz potential for the atom in the solid. The inverse mean free paths for volume excitations and the surface excitation parameters were established using the extended Drude dielectric function derived from optical data.

2.2. Monte Carlo simulations

The energy distribution of quasi-elastically backscattered electrons was studied using MC simulations. In these simulations, uniformly distributed random numbers were generated to determine the azimuthal and polar scattering angles and the pathlength between successive scatterings according to the differential and total elastic cross sections. Electrons were traced from their impinging points to the emerging points by recording all trajectories and energies in elastic scatterings. Each electron trajectory was recorded by the determination of the azimuthal and polar scattering angles and the pathlength between successive scatterings.

The probability density function of an electron scattered into the differential solid angle $\mathrm{d}\Omega$ after elastic scattering is determined by

$$P_\Omega(\theta, \phi)\,\mathrm{d}\Omega = \frac{\sin\theta}{\sigma_\mathrm{e}}\frac{\mathrm{d}\sigma_\mathrm{e}}{\mathrm{d}\Omega}\,\mathrm{d}\theta\,\mathrm{d}\phi, \tag{8}$$

where θ and ϕ are the polar and azimuthal scattering angles, respectively. It is assumed that the probability of elastic scattering is cylindrically symmetric with respect to the azimuthal angle. Applying the Poisson stochastic process, the probability density function of an electron with step pathlength Δs_i between the ith and $(i+1)$th scatterings is given by [30]

$$P(\Delta s_i) = \frac{1}{\lambda_\mathrm{e}}\exp\left(-\frac{\Delta s_i}{\lambda_\mathrm{e}}\right), \tag{9}$$

where $\Delta s_i = (z_{i+1} - z_i)/\cos\Theta_i$, Θ_i is the angle between the surface normal (inward direction) and the electron velocity after the ith scattering, and z_i and z_{i+1} are the depths of the electron at the ith and $(i+1)$th scatterings. Here Θ_i is related to Θ_{i-1} by

$$\cos\Theta_i = \cos\Theta_{i-1}\cos\theta_i - \sin\Theta_{i-1}\sin\theta_i\cos\phi_i. \tag{10}$$

When an elastic interaction occurs, the electron loses its energy by an amount equal to the Rutherford-type recoil energy. Thus the energy of electron after the ith scattering is given by

$$E_i(\theta_i) = \left(1 - \frac{4m}{M}\sin^2\frac{\theta_i}{2}\right)E_{i-1}(\theta_{i-1}), \tag{11}$$

where m and M are the mass of the electron and the atom, respectively. Note that equation (11) is valid for atoms at rest. To consider the thermal effect of atoms, the energy distribution of quasi-elastically backscattered electrons may be calculated by applying the single scattering model [31]. This model assumes a Maxwell–Boltzmann thermal velocity distribution of atoms. It also assumes that the recoil energy loss follows a Gaussian distribution with a maximum at the most probable value on the recoil energy loss for atoms at rest.

MC simulations trace electrons until either they are backscattered into the vacuum within acceptance angles or until their paths in the solid become so large that their intensity can be neglected. The intensity of quasi-elastically backscattered electrons is the average of the contributions from all (n) sampled trajectories, i.e. $I(E) = (1/n)\sum_{j=1}^{n}\Delta I_j(E)$. $\Delta I_j(E)$ may be obtained by tracing all step paths and recording recoil losses for the jth trajectory in elastic scatterings. In determining $\Delta I_j(E)$, however, the probability of an electron in any step pathlength without inelastic interaction should be considered. The probability density function without inelastic interaction in the step pathlength Δs_i is given by

$$P_i = \exp\left(-\frac{1}{\cos\Theta_i}\int_{z_i}^{z_{i+1}}\frac{\mathrm{d}z}{\lambda_i(E_i, z)}\right), \tag{12}$$

where $\lambda_i(E_i, z)$ is the depth-dependent electron inelastic mean free path. It is noted that $\lambda_i(E_i, z)$ is different for injected and ejected electrons [16]. In addition, the probability density function without surface excitation for an electron crossing the surface is given by $\mathrm{e}^{-P_\mathrm{s}(\alpha, E)}$, where α is the angle between surface normal in the outward direction and electron velocity [20]. Here, the surface excitation parameter may be calculated from [24] as

$$P_\mathrm{s}(\alpha, E) = \frac{1}{\cos\alpha}\int_{-\infty}^{0}\frac{\mathrm{d}z}{\lambda_i(E, z)}. \tag{13}$$

In the case of quasi-elastically backscattered electrons contributed by a single elastic scattering, for instance, the energy distribution may be written as

$$I_1(E)\,\mathrm{d}E = \frac{M}{2mE_0}\mathrm{e}^{-P_\mathrm{s}(\alpha_\mathrm{I}, E_0)}\int_{-\phi_\mathrm{A}}^{\phi_\mathrm{A}}\int_0^\infty \mathrm{e}^{-P_\mathrm{s}(\alpha_\mathrm{R}, E)} \times P_\Omega(\theta_1, \phi_1)F_\mathrm{I}(z_1)F_\mathrm{R}(z_1, \alpha_\mathrm{R})\,\mathrm{d}z_1\,\mathrm{d}\phi_1\,\mathrm{d}E, \tag{14}$$

where E_0 is the incident electron energy, α_I is the incident angle, α_R is the escape angle, ϕ_A is given by

$$\phi_\mathrm{A} = \begin{cases} \cos^{-1}\left(\dfrac{\cos\beta + \cos\alpha_\mathrm{I}\cos\theta_1}{\sin\alpha_\mathrm{I}\sin\theta_1}\right), \\ \quad \text{for } \pi - \alpha_\mathrm{I} - \beta \leqslant \theta_1 \leqslant \pi - \alpha_\mathrm{I} + \beta \\ \quad\quad \text{when } \beta \leqslant \alpha_\mathrm{I}, \\ \quad \text{for } \pi - \alpha_\mathrm{I} - \beta \leqslant \theta_1 \leqslant \pi + \alpha_\mathrm{I} - \beta \\ \quad\quad \text{when } \beta > \alpha_\mathrm{I}, \\ \pi, \qquad \text{for } \pi + \alpha_\mathrm{I} - \beta < \theta_1 \leqslant \pi \quad \text{when } \beta > \alpha_\mathrm{I}, \end{cases} \tag{15}$$

and β is the largest acceptance angle of escape electrons, i.e. $0 \leqslant \alpha_\mathrm{R} \leqslant \beta$. The probability density function of an injected electron reaching the depth z_1, at which elastic scattering occurs, without any inelastic interaction is given by

$$F_\mathrm{I}(z_1) = \frac{1}{\lambda_\mathrm{e}}\exp\left(-\frac{z_1}{\lambda_\mathrm{e}\cos\alpha_\mathrm{I}}\right) \times \exp\left(-\int_0^{z_1}\frac{\mathrm{d}z'}{\lambda_i^\mathrm{I}(E_0, z')\cos\alpha_\mathrm{I}}\right), \tag{16}$$

where $\lambda_i^\mathrm{I}(E_0, z')$ is the injected electron inelastic mean free path at depth z'. The probability density function of a reflected or ejected electron at depth z_1 to reach the surface without any inelastic interaction is given by

$$F_\mathrm{R}(z_1, \alpha_\mathrm{R}) = \exp\left(-\frac{z_1}{\lambda_\mathrm{e}\cos\alpha_\mathrm{R}}\right) \times \exp\left(-\int_0^{z_1}\frac{\mathrm{d}z'}{\lambda_i^\mathrm{R}(E, z')\cos\alpha_\mathrm{R}}\right), \tag{17}$$

where $\lambda_i^\mathrm{R}(E, z')$ is the ejected electron inelastic mean free path at depth z'. From equation (10), α_R is related to θ_1 by

$$\cos(\pi - \alpha_\mathrm{R}) = \cos\alpha_\mathrm{I}\cos\theta_1 - \sin\alpha_\mathrm{I}\sin\theta_1\cos\phi_1, \tag{18}$$

since $\Theta_1 = \pi - \alpha_\mathrm{R}$. Therefore, the energy distribution of quasi-elastically backscattered electrons contributed by a

single elastic scattering can be calculated using equations (11) and (14)–(18).

The quasi-elastic reflection coefficient may be defined as the integral of $I(E)$ for a range of electron energies according to

$$\eta(E_a, E_b) = \int_{E_a}^{E_b} I(E)\,dE. \tag{19}$$

2.3. Adjustments to measured spectra

There are two experimental factors that affect the energy spectrum of quasi-elastically backscattered electrons measured by a spectrometer. One of them is the energy distribution of the electron beam produced by an electron gun. The other is the energy resolution of the analyser of a spectrometer. To accommodate the consideration of these factors, it is assumed that both the energy distribution and the energy resolution are Gaussian functions. Let $G(\mu; \mu_0, \sigma)$ be the Gaussian function of a variable μ with the mean value μ_0 and the standard deviation σ. Considering the energy distribution of the electron beam, the intensity of quasi-elastically backscattered electrons may be obtained from

$$h(E) = \int_{-\infty}^{\infty} I(E + \omega - E_0)G(\omega; E_0, \sigma_g)\,d\omega, \tag{20}$$

where E_0 is the mean energy of incident electrons and σ_g is the standard deviation of the energy distribution. Further considering the energy resolution, the resulting intensity becomes

$$H(E) = \int_{-\infty}^{\infty} h(E')G(E; E', \sigma_r)\,dE', \tag{21}$$

where σ_r is the standard deviation of the energy resolution function. Substituting Gaussian functions into equations (20) and (21), one obtains the quasi-elastic spectra of backscattered electrons to be comparable of measured data.

3. Results and discussion

The MC method described above was applied to simulate the energy distribution of electrons quasi-elastically backscattered from Si and Au solids. The number of trajectories required in the simulations was around 10^8–10^9 in order to produce accurate results. The large number of trajectories was necessary because of the sharply peaked probability distribution toward small scattering angles. Although large-angle scattering events were seldom, any non-uniform sampling of them produced fluctuations in the energy spectra of quasi-elastically backscattered electrons. Figure 1 shows the results on simulated intensity (solid curves) of electrons elastically backscattered from Si for normally incident electrons of 5000 eV. Individual contributions from one, two, three, and all elastic scatterings are plotted separately. It is seen that this contribution decreases as the number of elastic scatterings increases. It is also seen that the elastic peak exhibits an energy shift (different from the incident energy) and an energy broadening.

Corresponding results calculated using equation (14) for a single scattering are plotted as dots. A comparison indicates

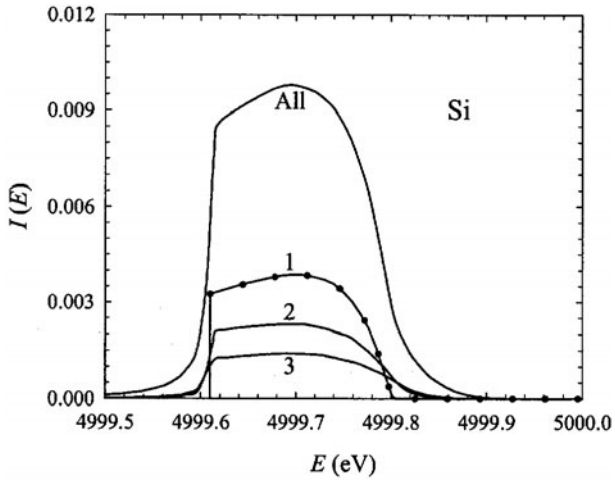

Figure 1. A plot of the MC simulation results on the intensity of electrons quasi-elastically backscattered from Si for normally incident electrons of 5000 eV. Individual contributions from one, two, three, and all elastic scatterings are plotted separately. Corresponding results calculated using equation (14) for a single scattering are also plotted (•) for comparison.

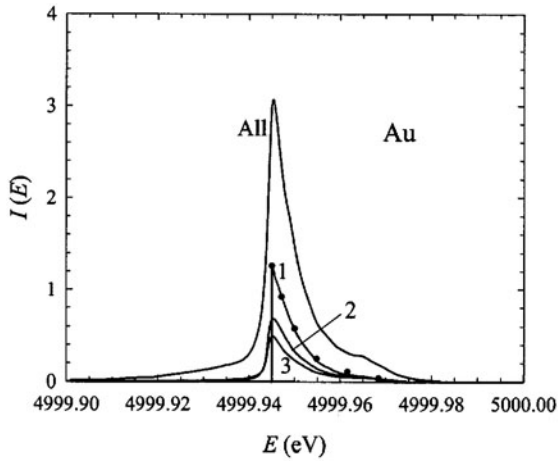

Figure 2. A plot of the MC simulation results on the intensity of electrons quasi-elastically backscattered from Au for normally incident electrons of 5000 eV. Individual contributions from one, two, three, and all elastic scatterings are plotted separately. Corresponding results calculated using equation (14) for a single scattering are also plotted (•) for comparison.

excellent agreement between data of MC simulations and equation (14). A similar plot of the energy distribution of electrons elastically backscattered from Au is shown in figure 2. It reveals that both the energy shift of the elastic peak and the recoil broadening of the peak energy are smaller for Au than for Si. This is due to the smaller energy loss for heavier atoms according to equation (11). The exact shape of the elastic peak depends on the elastic scattering cross sections of the solid studied.

Since incident electron energies are practically distributed with a Gaussian function around their mean value, the energy spectrum of the elastic peak depends on the full-width at half-maximum (FWHM) of the Gaussian function. Figure 3 plots the elastic peak for normally incident electrons of 5000 eV mean energy and two values of FWHM, 0.3 eV (solid curve)

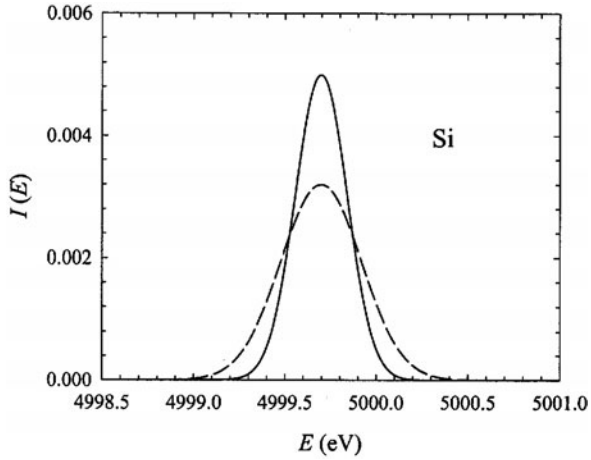

Figure 3. A plot of the MC simulation results on the intensity of electrons quasi-elastically backscattered from Si for normally incident electrons of 5000 eV mean energy and 0.3 eV (——) and 0.5 eV (- - - -) FWHM.

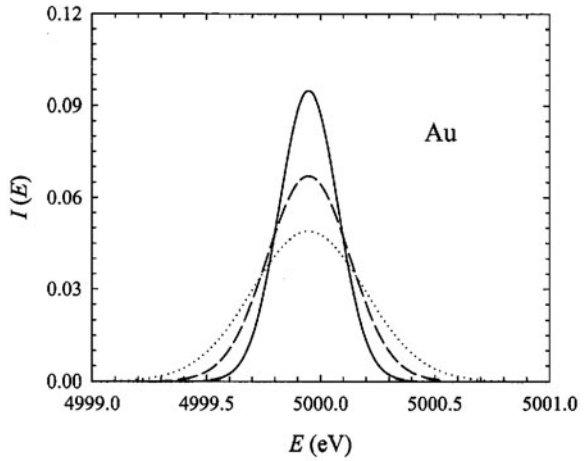

Figure 4. A plot of the MC simulation results on the intensity of electrons quasi-elastically backscattered from Au for normally incident electrons of 5000 eV mean energy and 0.3 eV FWHM. Spectrometer resolutions are 0 eV (——), 0.3 eV (- - - -) and 0.5 eV (· · · · · ·).

and 0.5 eV (dashed curve), in Si. The elastic peak is approximately a Gaussian function with an increased width. Such a width increase arises from the recoil broadening shown in figure 1. Therefore, the FWHM of the elastic peak is larger than that of the incident electron energy distribution.

Figure 4 shows the elastic peak in Au for two spectrometer resolutions, 0.3 eV (dashed curve) and 0.5 eV (dotted curve), with the same Gaussian energy distribution of 0.3 eV FWHM for incident electrons of 5000 eV mean energy. For comparison, the results considering no spectrometer resolution (solid curve) are also included. It is seen that the larger the FWHM of the spectrometer function the larger is the FWHM of the elastic peak. The FWHM of the calculated elastic peak is in good agreement with the prediction using $\Delta E_t = \sqrt{\Delta E_r^2 + \Delta E_g^2 + \Delta E_s^2}$ [27, 28], where ΔE_t, ΔE_r, ΔE_g and ΔE_s are, respectively, the FWHM of the resulting elastic peak, the recoil energy loss, the energy spectrum of incident electrons, and the spectrometer resolution function. In the

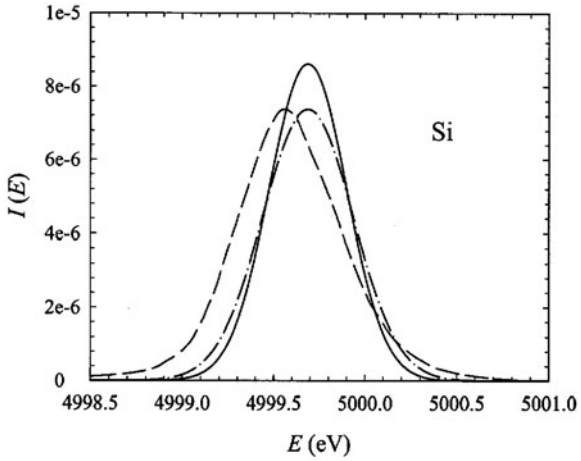

Figure 5. A plot of the MC simulation results on the intensity of electrons quasi-elastically backscattered from Si for normally incident electrons of 5000 eV mean energy and 0.4 eV FWHM. Here electrons are incident at an angle 50°; acceptance angles are between 0° and 3°; the spectrometer resolution is 0.28 eV. The thermal effect of atoms is neglected (— · —) and considered (——) by applying the single scattering model [31] with an FWHM of $\Delta E_T = 0.3$ eV at the room temperature. For a comparison, the experimental data (- - - -) [31] are also included.

case of normally incident electrons of 5000 eV in Si and Au, ΔE_r is 0.18 eV and 0.0048 eV, respectively, which is small compared with ΔE_g and ΔE_s applied in this work. Therefore, the resulting elastic peaks are approximately Gaussian distributions with widths mainly determined by ΔE_g and ΔE_s.

Figure 5 shows the results of calculated elastic peaks in Si with (solid curve) and without (chain curve) the consideration of the thermal effect of atoms. Here electrons of 5000 eV mean energy and $\Delta E_g = 0.4$ eV were incident at an angle of 50° with respect to the surface normal. The quasi-elastically backscattered electrons were collected with acceptance angles between 0° and 3°. For such a narrow range of acceptance angles, ΔE_r is very close to zero. The energy resolution of the spectrometer, ΔE_s, was set to 0.28 eV. The thermal effect was considered by applying the single scattering model [31] that assumed a Maxwell–Boltzmann distribution on the thermal velocity of atoms. The model also assumed that the recoil energy loss followed a Gaussian distribution with a maximum at the most probable value on the recoil energy loss for atoms at rest and with an FWHM of ΔE_T. Here the thermal effect was determined for the case of study by adopting a FWHM of $\Delta E_T = 0.3$ eV at the room temperature. It reveals in figure 5 that the elastic peak without the thermal effect shows a Gaussian distribution with a maximum at 4999.69 eV and an FWHM of 0.5 eV. The elastic peak with the thermal effect indicates a Gaussian distribution with a maximum at the same energy and a FWHM of 0.58 eV, in good agreement with the prediction using $\Delta E = \sqrt{\Delta E_T^2 + \Delta E_g^2 + \Delta E_s^2}$. For a comparison, the experimental data (dashed curve) [31] are also included in this figure. The minor deviation of the peak position between calculated results and experimental data is due to the fact that the recoil energy loss should be centred at the most probable value of this loss for vibrating atoms rather than for atoms at rest. Also, the thermal effect due to multiple elastic scatterings shifts the peak position and widens the peak. Both phenomena were not considered in the model.

4. Conclusions

MC simulations of the intensity distribution of electrons quasi-elastically backscattered from Si and Au have been performed by the consideration of the recoil effect in elastic scatterings. This effect resulted in a small energy shift and a certain broadening of the intensity distribution. In addition, the energy spectrum of incident electrons, the spectrometer resolution, and the thermal motion of recoil atoms all affected the shape and the FWHM of the distribution. Although these latter factors reduced and widened the distribution, they had no effect on the total intensity that depended on the interaction cross sections.

In this work, the intensity of electrons quasi-elastically backscattered from Si and Au was simulated for incident electrons of an energy distribution. The adjustment for the spectrometer energy resolution was allowed. Comparison of experimental data with MC simulated results with the inclusion of the thermal vibration effect of recoil atoms showed that both the peak position and the peak width of quasi-elastically backscattered electrons agreed quite well. The minor deviation in the peak position was due to the assumption that the recoil energy loss followed a Gaussian distribution with a maximum at the most probable value on the recoil energy loss for atoms at rest. In fact, the recoil energy loss should be centred at the most probable value of this loss for vibrating atoms rather than for atoms at rest. Also, the thermal effect due to multiple elastic scatterings could shift the peak position and widen the peak. Both phenomena are currently under study for the dependence of experimental geometry on the quasi-elastically backscattered spectra.

Acknowledgment

This research was supported by the National Science Council of the Republic of China under contract no NSC91-2215-E-009-065.

References

[1] Kirschner J and Staib P 1973 *Phys. Lett.* **42** 335
[2] Kirschner J and Staib P 1975 *Appl. Phys.* **6** 99
[3] Gergely G 1981 *Surf. Interface Anal.* **3** 201
[4] Jablonski A 1985 *Surf. Sci.* **151** 166
[5] Gruzza B and Pariset C 1991 *Surf. Sci.* **247** 408
[6] Jardin C, Gergely G and Gruzza B 1992 *Surf. Interface Anal.* **19** 5
[7] Dolinski W, Mröz S and Zagórski M 1988 *Surf. Sci.* **200** 361
[8] Beilschmidt H, Tilinin I S and Werner W S M 1994 *Surf. Interface Anal.* **22** 120
[9] Boersch H, Wolter R and Schoenebeck H 1967 *Z. Phys.* **199** 124
[10] Erickson N E and Powell C J 1989 *Phys. Rev.* B **40** 7284
[11] Laser D and Seah M P 1993 *Phys. Rev.* B **47** 9836
[12] Goto K and Shimizu R 1997 *Proc. Inter. Symp. Atomic Level Characterization for Materials and Devices '97* (Maui, Hawaii) *The Microbeam Anal*. vol 141 *Comp. Japan. Soc. Promotion Science* 1997, p 403
[13] Chen Y F, Kwei C M and Su P 1995 *J. Phys. D: Appl. Phys.* **28** 2163
[14] Jablonski, A Hansen H S, Jansson C and Touggard S 1992 *Phys. Rev.* B **45** 3694
[15] Kwei C M, Tsai S S and Tung C J 2001 *Surf. Sci.* **473** 50
[16] Kwei C M, Chiou S Y and Li Y C 1999 *J. Appl. Phys.* **85** 8247
[17] Jablonski A, Gryko J, Kraaer J and Touggard S 1989 *Phys. Rev.* B **39** 61
[18] Jablonski A 1991 *Phys. Rev.* B **43** 7546
[19] Jablonski A, Jasson C and Touggard S 1993 *Phys. Rev.* B **47** 7420
[20] Chen Y F, Su P, Kwei C M and Tung C J 1994 *Phys. Rev.* B **50** 17547
[21] Kwei C M, Su P, Chen Y F and Tung C J 1997 *J. Phys. D: Appl. Phys.* **30** 13
[22] Kwei C M, Chen Y F and Tung C J 1998 *J. Phys. D: Appl. Phys.* **31** 36
[23] Chen Y F and Kwei C M 1996 *Surf. Sci.* **364** 131
[24] Kwei C M, Wang C Y and Tung C J 1998 *Surf. Interface Anal.* **26** 682
[25] Kwei C M, Chen Y F, Tung C J and Wang J P 1993 *Surf. Sci.* **293** 202
[26] Kase K R and Nelson W R 1978 *Concepts of Radiation Dosimetry* (New York: Pergamon) p 68
[27] Tóth J, Varga D, Cserny I, Kövér L, Gruzza B, Zeze D, Jardin C and Gergely G 1998 *Vacuum* **50** 473
[28] Gergely G, Menyhard M, Benedek Z, Sulyok A, Kövér L, Tóth J, Varga D, Berényi Z and Tõkési K 2001 *Vacuum* **61** 107
[29] Sulyok A, Gergely G, Menyhard M, Tóth J, Varga D, Kövér L, Berényi Z, Lesiak B and Kosinski A 2001 *Vacuum* **63** 371
[30] Reimer L 1985 *Scanning Electron Microscopy* (New York: Springer) p 114
[31] Varga D, Tõkési K, Berényi Z, Tóth J, Kövér L, Gergely G and Sulyok A 2001 *Surf. Interface Anal.* **31** 1019